NASA-CR-201399

TTC-3452-R
19 June 1996
Copy No. 1

ThermoTrex Corporation

NASA AITP

Millimeter-Wave Passive Ultra-Compact Imaging Technology for Synthetic Vision & Mobile Platforms

Technical Report
Contract No. NCC1-203

First Year Report

Presented to:

NASA Center for Aerospace Information (CASI)
Attn: Accessioning Department
800 Elkridge Landing Road
Linthicum Heights, Maryland 21090-2934

Presented by:

ThermoTrex Corporation
Randall Olsen
10455 Pacific Center Court
San Diego, CA 92121-4339
(619)646-5300

This data was generated under NASA Cooperative Agreement NCC1-203. Any extraction from this report shall be marked.

TABLE OF CONTENTS

LIST OF FIGURES

1.0 FIRST YEAR TECHNICAL SUMMARY

This summary reports technical activities related to Contract NCC1-203 that took place during the months February 1995 through February 1996 at ThermoTrex Corporation (TTC) and at Aerojet Electronic Systems Division (Aerojet).

Substantial technical progress was made on all of the three high-risk subsystems of this program. The subsystems include dielectric antenna, G-band receiver, and electro-optic image processor. Progress is approximately on-schedule for both the receiver and the electro-optic processor development, while greater than anticipated challenges have been discovered in the dielectric antenna development. Much of the information in this report was covered in greater detail in the One-Year Review Meeting held at TTC on 22 February 1996. Most of the briefing view graphs of the review meeting are not repeated here, but can be provided on request.

1.1 DIELECTRIC ANTENNA

Before highlighting the challenges of the dielectric antenna it is helpful to review the performance goals of this project:

- Scan Angle - 20 degrees desired
- Loss - 6 dB end to end (3 dB average)
- Frequency - 206-218 GHz (6% bandwidth)
- Beam width - 0.25 degrees
- Length - 12 inches

The scan angle requirement was chosen to satisfy the needs of aircraft pilots. This requirement, coupled with the presently limited bandwidth processors (1 GHz state-of-the-art and 12 GHz in development in this program) forces the antenna to be dielectric (high scan angle air-filled waveguide-based antennas would be too lossy and their performance would vary too much as a function of frequency).

A high dielectric constant (e.g., 10) was initially chosen for the dielectric material. This choice lead to the following fabrication challenges:

- Total thickness variation (TTV) tolerance is 1 micrometer,
- Coupler spacing tolerance is 1 micrometer,
- Width tolerance is larger, but unknown,
- Surfaces must have mirror finish.

Also of importance is the difficulty in obtaining raw materials that satisfy the overall length requirement of 12 inches while simultaneously satisfying the above specifications.

Sapphire and silicon where initially selected as the most promising materials for the dielectric antenna. TTC and UCLA had previously succeeded in developing a sapphire antenna at 94 GHz so it was hoped that the technology could be pushed to the smaller dimensions needed for the present program. Unfortunately, the factor of two smaller cross-sectional dimensions required for 200 GHz operation are beyond the capabilities of all known sapphire processors (within the budget limits of this program). The scaling law that gives some appreciation for the difficulty is the cubic thickness dependence of the stiffness of an object. Thus, while we were reducing the cross section by only a factor of 2, the relative stiffness was reduced by a factor of 8. This increase in fabrication challenge, coupled with the 1 micron TTV tolerance, made sapphire fiber drawing impractical. Additionally, attempts to fabricate sapphire rods, starting from bulk raw materials have been fraught with machine tool and sapphire part breakage.

Due to the difficulties encountered with sapphire, most of our efforts have been applied to silicon. An important constraint for us in dealing with silicon is our requirement for ultrahigh purity silicon (to ensure low dielectric loss). This constraint limits the number of sources to one supplier in Denmark. If we could eliminate this constraint, a broad variety of semiconductor sources (including 8 inch diameter wafers) would have been available. Initially the flatness requirements appeared easily attainable. Our 1 micron flatness requirement is a rather loose tolerance compared with the optical world's ability to produced one-tenth wavelength (of light) or better (0.06 microns) surfaces. However, in our case, three additional constraints were added:

- The substrate was silicon (not glass) requiring special caustic polishing techniques,
- The substrate was very thin (0.25 mm), and
- The two surfaces of the substrate not only needed to be very flat, but also very parallel.

In spite of these difficulties, we succeeded in super-planarizing a number of high resistivity silicon wafers to less than 0.6 micron total thickness variation (TTV) over 4" diameter. This success also pointed out the importance of working with larger substrates. Though the TTV on individual specimens was under a micron, the specimen to specimen repeatability was spread over about a 5 micron band. In other words, if we were to try to make a 12" antenna by butt-coupling several specimens we would have to fabricate a very large number of specimens to produce matched thicknesses meeting our 1 micron thickness tolerance.

In other fabrication experiments we succeeded in slicing a boule of silicon in the axial direction to produce 3 cm wide by 0.25 mm thick (0.010") slices which were polished on two sides. These slices were further processed by diamond saw slicing to produce 0.25 mm by 0.25 mm (0.010" by 0.010") by 25 cm (10 inch) rods. These rods were only slightly shorter than the target 30 cm (12") due to breakage of the silicon boule during slicing (during which we learned that high resistivity is mechanically harder and more brittle than normal silicon). Millimeter wave experiments at 200 GHz with these rods revealed that waveguide to dielectric transitions were not reproducible (an unexpected

result based on 94 GHz experiments), whereas wider (up to 2 mm (0.075") slices displayed more reliable transitions. Although multi-moding is still a concern with these wide slices, we have established that sufficiently low loss dielectrics can be fabricated to meet the 0.2 dB/cm (0.5 dB/in) loss requirement.

We are currently attempting to extend the super-planarization method to silicon slabs of 25 to 30 cm (10 to 12 inch) length. Other issues yet to be resolved before building the first antenna element include:

- Development of a low loss transition,
- Establishment of a radiation coupler scheme which can meet the stringent dimensional tolerance requirements, and
- Completion of additional coupler measurements.

Due to the fabrication difficulties that have been uncovered, a number of alternatives are presently being explored including:

- An alumina rod-based design (which is an extrapolation on an antenna which EMS is developing for TTC for use at 94 GHz),
- A plastic dielectric H-guide design (for which we have commissioned Mission Research Corporation (MRC) to do preliminary design work),
- A dielectric slab antenna (which is in the conceptual stages presently), and
- An air-filled waveguide (solely for the purpose of enabling the demonstration of the entire imager system in the event no suitable dielectric antenna is produced in time).

1.2 G-BAND RECEIVER

Since our last report, Aerojet has succeeded in reducing the double side-band noise figure for the mixers from 11 dB to 7 dB which surpassed the goal of 8 dB. This record breaking mixer noise-temperature performance is particularly satisfying with regard to its extremely low local oscillator (LO) power requirement. This is important because more than one mixer can be driven by an LO thus enabling lower component costs for future systems.

Three whiskerless mixer diodes fabricated at the University of Virginia were evaluated. This type of diode is of interest because it is suitable for large scale manufacturing.

Using a state-of-the-art CAD system, Aerojet successfully designed the mechanical layout and interfaces for 0.25" -wide stackable thin mixers. The computer files for the input interface are expected to aid the design and fabrication of the antenna subsystem.

The high pass filter has proved to be the most difficult unit within the receiver subsystem. Theoretical work has provided two designs that have been executed as hardware. Unfortunately, the experimental measurements have shown much weaker filtering than needed to satisfy the system requirement of reducing the lower side band by 20 dB. The lack of satisfactory performance apparently stems from difficulty in attaining the tight tolerances required for a cosine shaped taper in the filter. Work in this task will continue from both design and fabrication perspectives.

1.3 ELECTRO-OPTIC (EO) PROCESSOR

A 1-channel EO processor has been successfully demonstrated. The objective of steering a laser beam by tuning a frequency generator between 6 GHz and 18 GHz was shown. Furthermore, the resolution goal of 100 MHz, or 120 spots was achieved. During the recent months, the task of removing the carrier and lower side-band from the modulated light output was addressed by adding a holographically produced grating (2,200 line per mm) to the optical bench upstream from the analyzing etalon. The grating spread the various frequencies sufficiently to enable a mirror edge to remove the unwanted signals (the carrier is reduced by more than 13 dB).

Hardware and software have been developed for real time compensation for optical phase drifts. This system has been demonstrated for an 8 channel array for two modes: start-up and continuous duty. On start-up, the system initially turns off all channels except a single pair. The relative phase of one channel is varied and the magnitude of the light corresponding to a central image spot is monitored to determine the proper phase. Additional channels are turned on one at a time, and their phases varied to produce the brightest central peak. This procedure can phase align all channel in about one second. A second procedure has been developed with the aim of correcting phase changes as rapidly as once every 1/30th of a second. While the first procedure is fully operational, the second is only partially functional at this time. It is presently suspected that polarization effects may be causing tracking difficulties with the faster procedure. Therefore, experiments will be performed to determine the cause and seek full operationality of the faster procedure. Since the optical system has turned out to be more phase stable than expected, phase tracking may actually be performed in an on-going basis by the first procedure. [Note: by the date of report submission, the faster procedure has been made operational.]

A purpose-built CCD camera with large full-well capacity (providing better statistics than possible with conventional cameras) has been built, tested and recently received at TTC.

Harris Corporation is five months into a ten month contract to develop a 32 channel modulator array. Several elements of the integrated device have already gone through design, modeling, fabrication and testing. An eight channel test array will be delivered to TTC in about one month.

2.0 FINANCIAL ACTIVITY SUMMARY

This summary reports financial activity relating to NASA Contract NCC1-203 that took place during the months of February 1995 through January 31, 1996 at TTC and at Aerojet Electronic Systems Division. (See Tables 1 and 2.)

Allowing for fully-committed subcontract dollars to UCLA and UVA, all tasks show nominal budget vs. schedule tracking with the exception of Tasks 3, 6, and 7 at TTC and Tasks 11, and 13 at Aerojet.

Task 3 is actually showing nominal budget vs. schedule tracking assuming that Harris delivers a subsystem which requires very little integration cost. The cost growth for Task 3 is an estimation for such integration cost. Tasks 6 and 7 relate to the subsystem which has presented the greatest level of unanticipated challenges. Cost growths for Tasks 3, 6 and 7 correspond to amounts which were not invoiced for matching funds on Tasks 1 and 4.

Tasks 11 and 13 have been completed at a cost of just $183,100 vs. a budgeted amount of $350,000 producing a savings of $166,900.

2.1 PUCI TECHNOLOGY DEVELOPMENT SCHEDULE

The following schedule indicates that nearly all tasks are close to tracking our original estimate plus a one to two month stretch by the 18 month. The tasks of greatest concern are 6 and 7 on dielectric antenna development. Contingencies are being considered in the event that technical progress does not meet our original goals with regard to antenna performance. If necessary a de-scoped antenna will be built to enable demonstration of all of the three technologies that have been developed in this program.

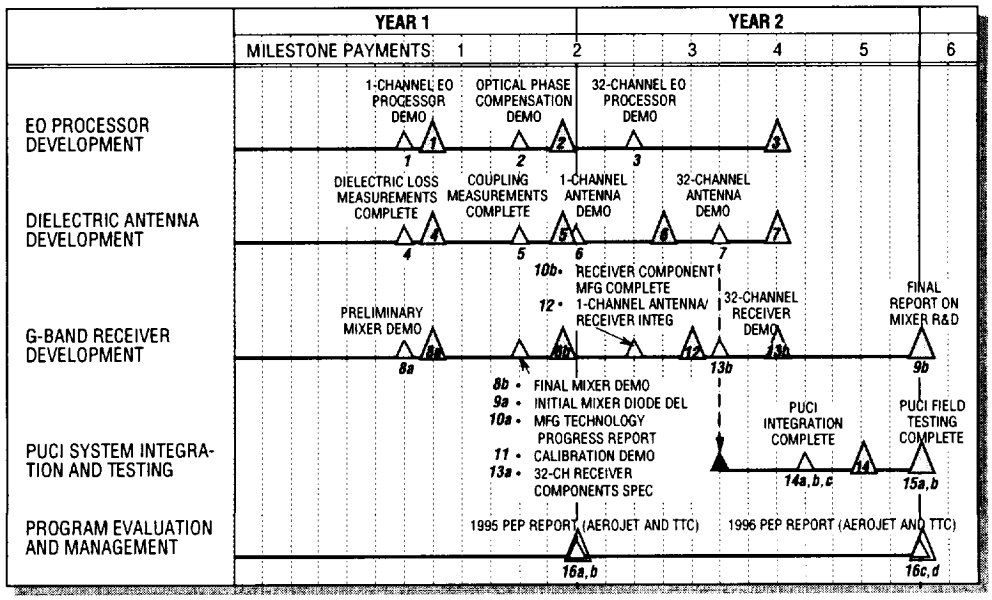

TTC TASKS UNDER NASA COOPERATIVE AGREEMENT NO. NCC1-203

As of January 31, 1996

TASK	DESCRIPTION	BUDGET	AMT SPENT COMMITTED	% SPENT	% WORK COMPLETED	EST. TO COMPLETE	TOTAL COST	NASA COST MATCH	MILESTONE PYMT PERIOD	MILESTONE INVOICE DATES
1	1 Channel EO Processor	$260,000	$194,880	75%	100%	$0	$194,880	$0*	1	October`1995
2	EO Phase Compensation	$130,000	$90,080	69%	100%	$0	$90,080	$45,040	2	February`1996
3	32 Channel EO Processor	$450,000	$444,533	99%	40%	*$150,000*	*$594,533*	*$297,267*	4	September`1996
4	Dielectric Loss Measurement	$120,000	$137,990	115%	100%	$0	$137,990	$0*	1	October`1995
5	Antenna Coupling Measurement	$120,000	$138,526	115%	100%	$0	$138,526	$69,263	2	February`1996
6	1 Channel Antenna	$120,000	$120,015	100%	50%	*$120,000*	*$240,015*	*$120,007*	3	June`1996
7	32 Channel Dielectric Antenna	$170,000	$73,786	43%	20%	*$230,000*	*$303,786*	*$151,893*	4	September`1996
14a	PUCI Intergration	$210,000	$0	0%	0%	$210,000	$210,000	$105,000	5	December`1996
15a	PUCI Field Test	$225,000	$0	0%	0%	$225,000	$225,000	$112,500	6	March`1997

NOTES:

1) * Denotes no cost matching invoiced for these milestones (Consideration received for projected cost growth in tasks 3, 6, & 7, milestone payment periods 3 & 4)

2) *Italic* formatting used to denote estimate

AEROJET TASKS UNDER NASA COOPERATIVE AGREEMENT NO. NCC1-203

As of December 30, 1995

TASK	DESCRIPTION	BUDGET	AMT SPENT COMMITTED	% SPENT	% WORK COMPLETED	EST. TO COMPLETE	TOTAL COST	NASA COST MATCH	MILESTONE PYMT PERIOD
8a	Preminminary Mixer	$100,000	$33,300	33%	100%	$0	$33,300	$16,650	1
8b	Upgraded Mixer	$75,000	$110,500	147%	100%	$0	$110,500	$55,250	2
9a	Mixer Diodes	$75,000	$130,000	173%	100%	$0	$130,000	$65,000	2
9b	Upgrade Diodes	$75,000	$0	0%	0%	*$75,000*	*$75,000*	*$37,500*	6
10a	MFG Technology	$100,000	$46,300	46%	100%	$0	$46,300	$23,150	2
10b	Receiver Component	$85,000	$0	0%	0%	*$85,000*	*$85,000*	*$42,500*	3
11	Calibration Demo	$50,000	$200	0%	100%	$0	$200	$100	2
12	1-Channel Ant./Rec.	$100,000	$600	1%	1%	*$99,400*	*$100,000*	$50,000	3
13a	32-Channel Rec. Spec.	$300,000	$182,900	61%	100%	$0	$182,900	$91,450	6
13b	32-Channel Rec. Demo	$400,000	$0	0%	0%	$400,000	*$400,000*	*$200,000*	4
14b	PUCI Sys Integration	$100,000	$0	0%	0%	*$100,000*	*$100,000*	*$50,000*	5
15b	PUCI Field Test	$100,000	$0	0%	0%	*$100,000*	*$100,000*	*$50,000*	6
16b	Year 1 Mgmt	$40,000	$19,800	50%	88%	*$10,000*	*$29,800*	*$14,900*	6
16d	Year 2 Mgmt	$40,000	$0	0%	0%	*$40,000*	*$40,000*	*$20,000*	3

3.0 TECHNICAL ACTIVITY SUMMARY

Substantial technical progress was made on all of the three high-risk subsystems of this program. The subsystems include dielectric antenna, G-band receiver, and electro-optic image processor. Progress is approximately on-schedule for both the receiver and the electro-optic processor development, while greater than anticipated challenges have been discovered in the dielectric antenna development. Much of the information in this report was covered in greater detail in the One-Year Review Meeting held at TTC on 22 February 1996. Most of the briefing view graphs of the review meeting are not repeated here, but can be provided on request.

3.1 TASK 1 - 1 CHANNEL EO PROCESSOR DEMONSTRATION

The objective of this demonstration is to steer a laser beam in one direction by tuning a frequency generator between 6 GHz and 18 GHz. The frequency resolution goal set out in the statement of work is 100 MHz, which would produce 120 resolvable spots over the 12 GHz bandwidth. These goals were completed on September 6, 1995 and reported on in a previous technical report. The experimental set-up has been upgraded since that time, however, and is described here.

The single channel layout is pictured in Figure 1. The SDL 5411 diode laser previously used has been replaced with a fiber coupled SDL 5710 DBR laser which has high frequency stability. This diode laser is fiber coupled to a UTP EO amplitude modulator which operates up to 18 GHz. The output of this modulator is collimated and reflected off a diffraction grating described below. The light is then brought to an intermediate focus at a mirror/beam stop before being directed into an etalon. The Burleigh TL-38 etalon has a free spectral range of 12 GHz and a finesse of approximately 120. This produces a frequency resolution capability of 100 MHz full-width half-maximum. The light which passes the etalon is then focused onto the video camera. The horizontal position of the spot in the resultant image indicates the frequency of the light. Modulation frequencies from 6 GHz to 18 GHz span the image.

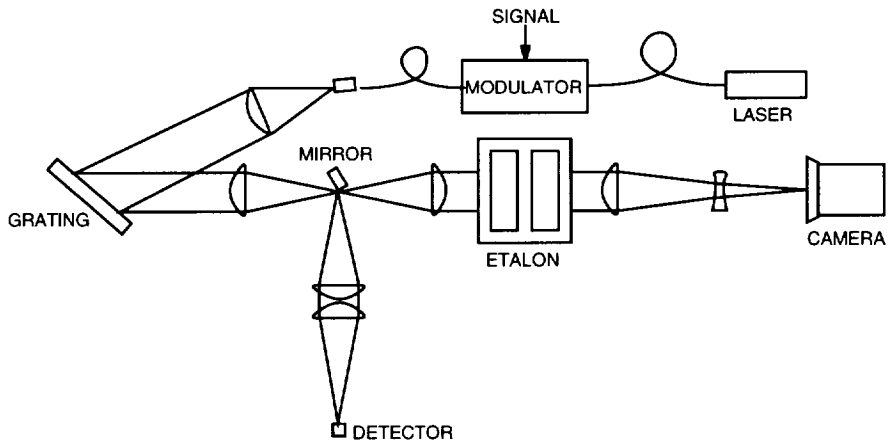

- Upper sideband routed through etalon
- Carrier routed to detector

Figure 1. Single channel EO processor demonstration.

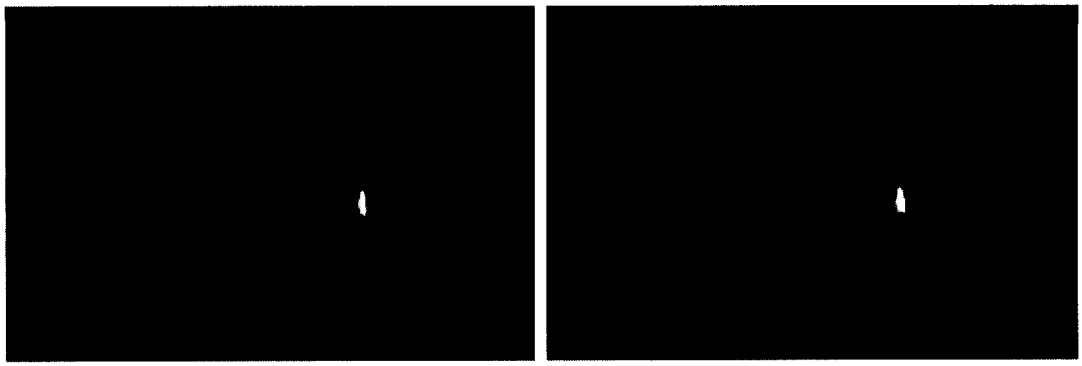

8.9 GHz MODULATION 9 GHz MODULATION

Figure 2. Showing 100 MHz resolution over 12 GHz.

The frequency resolution capability of the system is shown in Figure 2. The first image is of a spot produced by a modulation signal of 8.9 GHz. The modulation frequency was stepped to 9 GHz to produce the second image. A marker has been affixed to the screen to show relative position. The 100 MHz shift in frequency results in a position shift equal to the half power width of the spot.

An issue left unresolved in the earlier implementation was the effect of the carrier beam and lower sideband on the image. When the laser beam is modulated with a microwave signal, light is shifted to frequencies both above and below the original laser frequency. A portion of the light also remains at the laser frequency as the carrier beam. The information required by the processor is contained in only the upper sideband, so the carrier and the lower sideband must be filtered out. An etalon with a free spectral range of 12 GHz will alias these components into the image, and an increase in the free spectral range of the etalon would result in a decrease in frequency resolution. Therefore, the unwanted spectral components are filtered before the etalon by a diffraction grating.

The diffraction grating which filters the carrier and lower sidebands, as shown in Figure 3, is a Spectrogon holographically produced grating. It has 2,200 lines per millimeter, is 50 x 50 mm, and has a gold coating for better than 90% efficiency. There is a 6 GHz separation between the carrier and upper sideband which equates to an angular separation of 1.33×10^{-4} rad exiting the grating at 76°. Based on the width of the grating, this angular separation is $1.88\ \lambda/d$, a margin by which the components are mostly separable. The light from the diffraction grating is focused to a plane where a mirror is used to deflect the unwanted components away from the etalon so they do not intrude on the image. The upper sideband light continues through the etalon and onto the camera. The intensity of the carrier frequency light reaching the camera is reduced by more than 13 dB with the mirror in place (see Figure 4).

SPECTROGON HOLOGRAPHIC GRATING

GROOVE FREQUENCY	2200 G/mm
COATING	GOLD
SIZE	50 x 50 x 10 mm

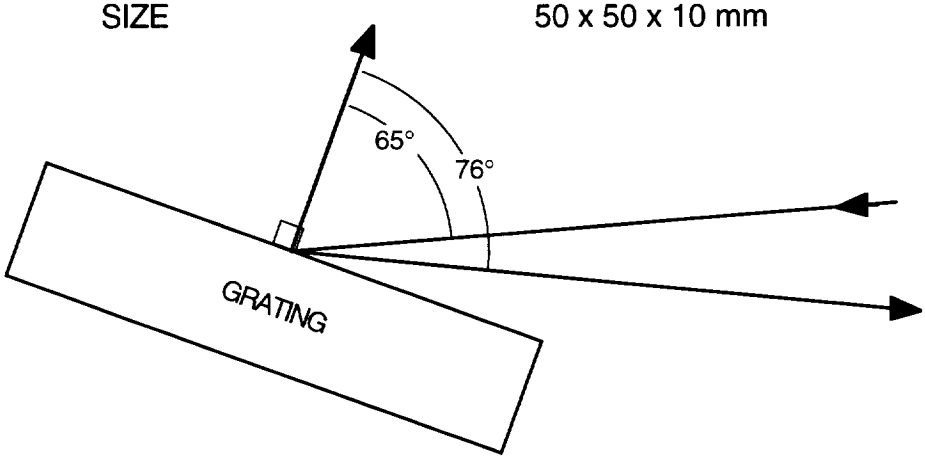

$$\Delta\angle @\ 6\ \text{GHz} = 1.33 \times 10^{-4}\ \text{rad} = 1.88\ \frac{\lambda}{d}$$

Figure 3. Diffraction grating which blocks the carrier and lower sidebands.

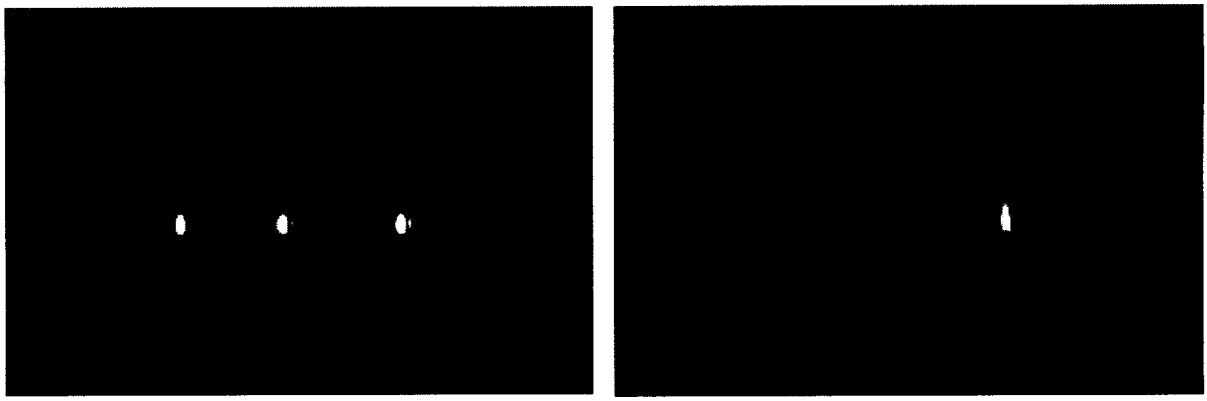

Figure 4. Showing blocking of carrier and lower sideband.

3.2 TASK 2 - MULTI-CHANNEL REAL TIME OPTICAL PHASE COMPENSATION

The goal of this task is to develop hardware and software for real-time active phase compensation of differences in relative phase lengths of fiber optic channels in a phased array. This task was completed as of February 27, 1996 with the implementation of a phase compensation system to instantaneously correct path length differences in an eight channel optical phased array.

A multi-channel electro-optic processor processes phase by imparting the phase of a microwave signal to the phase of an optical signal and interfering the optical signals of the various channels. For this approach to work, the relative phase lengths of all the optical channels must be equal, to a factor of 2π, and must be kept constant. In the distance from the first split of laser light to the launch in free space, each channel is susceptible to a path length shift relative to other channels. A phasing requirement of $\lambda/20$ equates to a sensitivity of less than 40 mm in fiber. The current demonstration system of eight channels is relatively stable in a lab environment, taking approximately 15 minutes to degrade from a phased state to an unphased state. Air flow around the exposed fibers, however, hastens the phase degradation, and the heat from placing one's hands near the fiber causes the phased state to degrade in approximately one second. The current system has 20 cm of exposed fiber and 50 cm of protected fiber in each channel. The exposed fiber has greater sensitivity to thermal variations than the protected fiber. Ideally, the 32 channel system being developed by Harris will have no fiber, exposed or otherwise, only about 3" of integrated optical waveguide for each of 32 channels on a single chip. Thus the new system will be less susceptible to phase disturbances than the current system. Nevertheless, some system of active phase compensation will still be required.

The phase compensation system consists of a 486 PC with a C30 processor board which receives data from an amplified photodiode and sends control voltages to the modulator array. The carrier signal from each channel of a multi-channel array is deflected to a photodiode by a mirror located at an intermediate focus "phase control set-up" (see Figure 1). The carrier signals interfere in the plane of the photodiode, producing a bright spot on the diode when all channels are in phase. If some channels are out of phase, the power on the photodiode is less. The signal on the photodiode is transferred to the phase control board, which sends appropriate control voltages to the modulator array. Each optical channel in the modulator array has a low frequency phase modulator, in addition to the high frequency modulator, which can be shifted through 2π to correct the phase length of the channel. A DC voltage to these modulators sets the phase of each channel. An 1 MHz voltage can also be applied to dither the phase around its DC setting. When all channels are in phase, the photodiode response at 1 MHz from such a dithering should be zero. The intensity of each channel also can be switched off and on by changing the amplitude modulator bias voltage.

The phase control board with C30 processor, pictured in Figure 5, controls all the output voltages. The board samples both 1 MHz AC and DC components of the signal from the photodiode at 10 MHz. The C30 then extracts the levels of these signals and uses the information to set D/A chips which provide output phase voltages. The C30 also provides a 1 MHz square wave, filtered to a sine wave, which can be added to the phase output voltages. The 486 PC is used to control the user interface with the system.

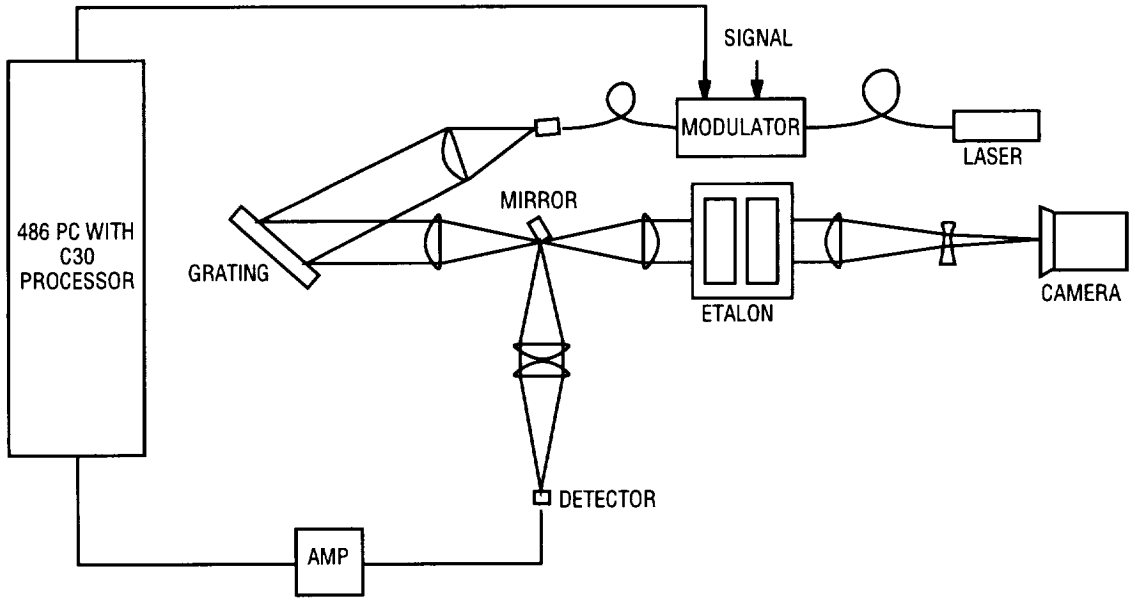

Figure 5. Schematic of phase control system.

Two separate algorithms are used to control the phases of the optical channels. The first algorithm is to be used on start up of the system, when all the channels have random phasing relationships. This algorithm turns off all but the first two channels and steps channel two through all possible phase settings, measuring DC photodiode response at each step. The channel two phase is then set to the phase setting which produced the highest level. Channel three is then turned on and stepped through all phase settings and set to the level which produces the highest level. This process is repeated for each channel until all channels are in phase with one another. The second algorithm is to be used after the first algorithm to dynamically correct for phase disturbances. This algorithm steps through all the channels, performing the following steps at each channel: Add a 1 MHz AC component to the DC phase control voltage; measure AC and DC responses at the photodiode; step the phase control voltage up and down one step from its current setting; measure AC and DC photodiode responses at each of these settings; set the phase control voltage to the setting which produced the highest DC and lowest 1 MHz AC responses; turn off the 1 MHz AC component; move to the next channel. In this manner, the algorithm makes small corrections for phase disturbances. The algorithm is capable of correcting 32 channels in less than 1/30 of a second.

The phase compensation system includes a user interface to set variables such as number of channels to be controlled, correction speed, comparison tolerance levels, and phase step size. The interface also has a data logging utility so the user can monitor the decision making process used by the algorithm. Used together, these features allow for debugging and optimization of the phase control system.

The phase compensation system is currently being demonstrated on an eight channel electro-optic modulator array. Unmodulated light from the eight channels interferes on a photodiode providing feedback to the system as well as a camera so that the phasing of the channels can be observed. Figure 6 shows the interference pattern of the eight channels with random phase relationships. Figure 7 shows the interference pattern after the initial phase compensation routine was run. The channels now form a distinct spot, as well as sidelobes resulting from the sparse array. The initial phase compensation routine consistently returns unphased channels to a phased state. The continuous phase correction routine will retain that state in most circumstances. Occasionally, noise or environment disturbs the system in such a manner that the correction routine will not cause the channels to re-converge to a phased state. In that case, the initial phase compensation routine must run again. TTC will continue to refine the phase compensation system in the remainder of the contract to improve the performance of this dynamic correction routine. [Note: by the date of report submission, the faster procedure has been made operational.]

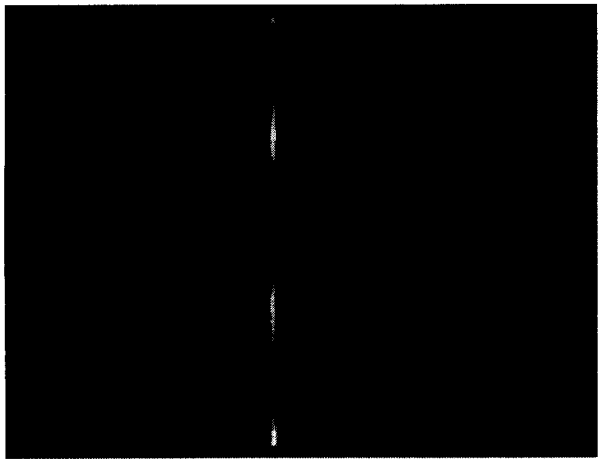

Figure 6. Interference pattern of eight channels with random phase relationship.

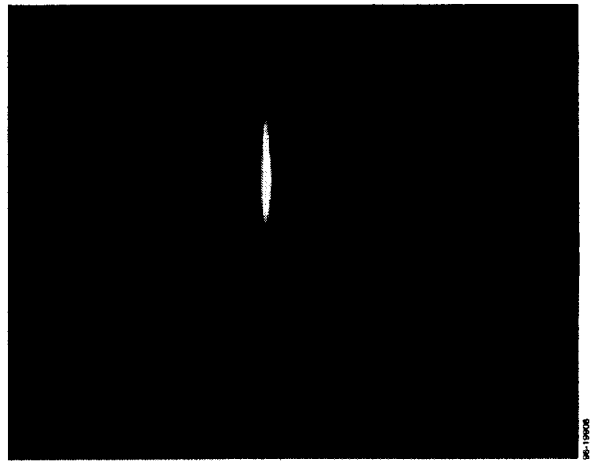

Figure 7. Interference patterns after phase compensation.

3.3 TASK 3 - MULTI-CHANNEL ELECTRO-OPTIC PROCESSOR DEMONSTRATION

Work is continuing on the goal of developing a phased-array optical processor for instantaneous processing of frequency and relative phase information from an array of microwave signals.

Harris Corporation is in the fifth month of a ten month contract to develop a 32 channel modulator array for this task. This modulator array will be implemented on a single substrate of $LiNbO_3$, as opposed to using separate substrates for each modulator. Coupling to and from the substrate will be done via GRIN rod lens arrays rather than with fibers. Advantages of this novel approach include less susceptibility to relative phase errors, more efficient optical coupling, and lower cost of long-run production. Because the electrodes for each modulator lie on the same substrate, extensive work is being done to isolate the signal feeds to limit electrical crosstalk. The SDL 5700 series DBR diode laser, rather than the 5400 series laser, has been identified as the light source for the modulator array. This laser provides the necessary power of 100 mW in a stable single longitudinal mode. A lower than specified loss in the IO modulator array allowed the use of a lower power laser than originally anticipated. Harris Corporation will integrate the laser into the modulator input.

Harris Corporation has currently completed the waveguide design and the electrical modeling of the modulators using a 3-D finite element code (Hewlett-Packard HFSS). A mask is being fabricated for an eight channel test piece which will be delivered to TTC in approximately one month. Delivery of the full thirty-two channel array is expected in August.

The Photometrics CCD camera to be used in the processor has been tested and delivered to TTC. Measured specifications of the camera include: 512 x 512 pixels; 184,000 electron full well capacity; 29.3% quantum efficiency at 850 nm; 2 x 2 pixel on-chip binning; 14.2 Hz readout rate in 256 x 256 mode. The frame transfer readout from the camera will be passed via a custom interface to an Alacron i860 processor.

The photon budget of the electro-optic processor has been an ongoing concern due to the fact that low processor noise requires high light levels at the camera. The laser diode selected by Harris Corporation provides a maximum of 100 mW single mode output at 852 nm. Using the above specifications of the Photometrics camera, expected losses in the etalon and other free space optics, and the anticipated 12 dB maximum loss in the integrated optical modulator, the required laser diode power for camera saturation is under 100 mW.

3.4 TASK 5 - DIELECTRIC ANTENNA COUPLING MEASUREMENTS

The objective of this task is to identify a suitable waveguide perturbation method to enable radiation coupling to the dielectric waveguide and to determine the parameters that affect the coupling coefficients of the radiators. An array of periodically spaced metal grating elements above the dielectric waveguide was chosen as the radiating elements. Metal patches above the guiding rod results in radiation with the polarization perpendicular to the guiding direction. The metal grating elements are formed by photolithographically etching away excess metal from Cuflon (copper coated Teflon).

The spacing between two adjacent metal patches determines angle of mainbeam radiation as a function of frequency. The coupling coefficients of the patches can be controlled by varying the width of the patch along the direction of the waveguide. The greater the patch width, the greater the coupling coefficient will be. The coupling coefficient can also be increased by orienting the Cuflon so that the metal patches, instead of being above the Teflon as shown in Figure 8 (a), are

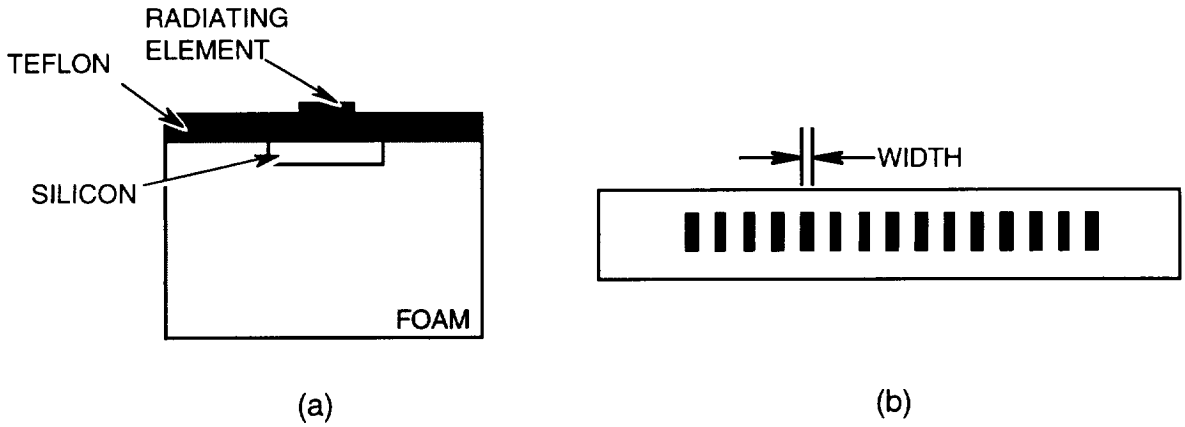

Figure 8. Geometry for coupling measurements.

directly on top of the silicon rod and underneath the Teflon layer. To achieve a uniform aperture illumination in the final antenna, the coupling of the patches closest to the feed end of the antenna must be very small, while the coupling of the patches near the load end must be large.

Coupling coefficients are experimentally determined by measuring the losses due to radiation from different arrays of identical metal elements. The transmitted power through a waveguide with a particular grating is measured and compared against the power through a waveguide without any metal gratings. The coupling coefficient from a single grating element is then unfolded from the measured power difference. UCLA received delivery of a 200 GHz power source in December, and preliminary antenna coupling measurements were performed at the UCLA Millimeter Wave Laboratory. These measurements showed that an array of 75 metal patches with dimensions of 0.51 mm x 0.10 mm (20 mil x 4 mil) and a periodic spacing of 0.64 mm etched from a 0.25 mm (10 mil) thick piece of Cuflon resulted in a radiation loss of 2 dB across the 206 - 218 GHz band. The silicon rod used had a cross section of 1.65 mm x 0.25 mm (65 mil x 10 mil), and the metal grating was on the top surface of the Teflon. By reversing the Cuflon layer so that the metal grating is directly above the silicon, the radiation loss increased by 8 dB. Increasing the metal patch size to 0.51 mm x 0.25 mm (20 mil x 10 mil) of the grating above the Teflon also increased the radiation coupling, giving a total radiation loss of 5 dB. Unfolding slot conductance from these transmission measurements results in individual conduc-

tances of 0.0002 and 0.0048 for the 0.10 mm (4 mil) and 0.25 mm (10 mil) wide patches above the Cuflon, respectively, and 0.0124 for the 0.102 mm patches below the Cuflon.

These measurements give rough empirical scaling curves for coupling vs. patch width and proximity to the feedline. To achieve a uniform antenna aperture, the coupling as a function of patch element is shown in Figure 9 for an antenna with 476 radiating elements spaced 0.64 mm apart. A waveguide loss of 0.2 dB/cm (0.5 dB/inch) and a 5% power to load in transmit mode is assumed.

The first element requires a conductance of 0.0008 and the last element requires a conductance of 0.0151. Based on the preliminary measurements, this will result in our using slots ranging from approximately 0.1270 mm (5 mils) wide placed above the Teflon at the feed end of the antenna to slots 0.1270 mm placed below the Teflon at the load end.

When final waveguide dimensions are chosen for the single channel antenna, these measurements will be repeated to better characterize the appropriate coupling ranges for the final antenna. Additionally, work is currently underway to improve the metal waveguide to dielectric waveguide transitions in order to improve the precision of these measurements.

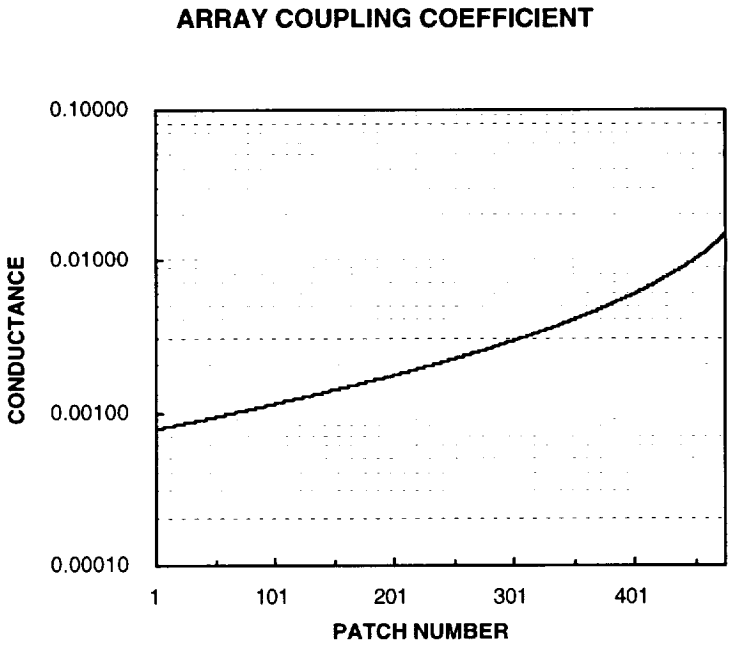

Figure 9. Theoretical coupling for the geometry of Figure 8.